# Dalton Transactions

Accepted Manuscript






ROYAL SOCIETY OF CHEMISTRY

www.rsc.org/dalton

Journal Name

ARTICLE

# Synthesis and structural characterisation of transition metal fluoride sulfates†

Received 00th January 20xx,
Accepted 00th January 20xx

DOI: 10.1039/x0xx00000x

www.rsc.org/

Kayleigh L. Marshall[a], Qianlong Wang[a], Hannah S. I. Sullivan[a] and Mark T. Weller[a]

Eleven first row transition metal fluoride sulfates synthesised in hydrofluorothermal conditions have been structurally characterised by single crystal X-ray diffraction and exhibit a wide variety of structural motifs. The polyionic structures containing Ti, V, Mn and Fe vary from discreet polyhedral units in $Na_4TiF_4(SO_4)_2$ and $[N_2C_{10}H_{12}]$ $TiF_4SO_4$, through one dimensional chains in $(K_2FeF_3SO_4$, $Li_3FeF_2(SO_4)_2{\cdot}H_2O$, $Li_{1.87}Ti_{1.13}O_{0.39}F_{1.61}(SO_4)_2$, $[N_2C_{10}H_{12}]TiF_2(SO_4)_2$, $[N_2C_6H_{16}]Fe(SO_4)_2F$ and $[N_2C_6H_{16}]V(SO_4)_2F)$, and to two dimensional layers in $([N_2C_6H_{16}]^{2+}Mn_2F_2(SO_4)_2$, $Na_2VF_3SO_4$ and $Na_3CrF_2(SO_4)_2)$.

## Introduction

Inorganic materials formed through the connectivity of polyhedral units containing metal centres and tetrahedral oxopolyhedra (e.g. $PO_4$, $AlO_4$, $SiO_4$ and $SO_4$) have a variety of potential and actual applications which arise from their structures and compositions.[1-3] These applications include those as catalysts[2], ion exchangers and gas storage/adsorption media.[4] Such functionalities are the result of rigid and stable frameworks formed from interlinked polyhedra with accessible inter-framework space, such as that between layers or in pores as seen in aluminosilicate zeolites.[4] When $Li^+$ or $Na^+$ cations are included in the inter-framework space, in combination with a redox active transition metal, they may be highly mobile and de-intercalated electrochemically and so the material may have applications systems as the anode or cathode in a rechargeable Li or Na battery.[5, 6] Where the framework metal is redox inactive potential applications arise as the electrolyte in a fully solid state battery. In respect of battery cathode materials, the inclusion of fluoride into the polyanionic framework has been shown to increase the cell potential through inductive effects and, thereby, lead to increased cell capacity.[7-9] Incorporation of fluoride may also enhance cation mobility by reducing electrostatic interactions along conduction channels. Therefore, there is considerable demand from electrochemists for new materials of this type for battery material characterisation.

Recent research in this field has led to the discovery of a number of mid- to late- first row transition metal fluorophosphate and fluorosulfate frameworks, as previously published.[10-16] The inclusion of larger cations, such as potassium or molecular templating cations, has been commonly used to enhance the open nature of framework materials, which can be favourable for fast ion transport and hence for battery performance[17], though it leads to potential applications in molecular sieving. For the early- to mid- first row transition metals relatively few fluorophosphate and fluorosulfate compounds have been described, though related materials, particularly for titanium, are of interest as solid state battery anodes. For example $NaTi_2(PO_4)_3$ has been studied as a sodium ion battery anode.[18-20]. In this work we present recent results of a systematic study into the synthesis of early first row transition metals in combination with fluoride and sulfate anions.

## Results and discussion

A summary of the compositional and structural data for the eleven phases reported in this article is shown in Table 1. A full discussion of their synthesis and determined structural features is detailed in the following sections.

### (I) $Na_4TiF_4(SO_4)_2$

Colourless, prismatic crystals of $Na_4TiF_4(SO_4)_2$ were grown from the mixture of $TiF_3$ (0.10407 g, 1 mmol), NaF (0.12614 g, 3 mmol) and $H_2SO_4$ (0.280 mL, 5 mmol) treated hydrothermally at 200 °C for 96 hours. Visual 90% phase purity confirmed by PXRD (see supporting information). Compound **I** crystallises in the triclinic space group P-1 and contains an unusual discreet complex polyanion $[TiF_4(SO_4)_2]^{4-}$ constructed from one $TiF_4O_2$ octahedron which shares its two *trans* oxygen atoms with two $SO_4$ tetrahedra. Sodium cations separate these discrete polyanionic units which align above one another along each of the unit cell dimensions. Two distinct $Na^+$ environments exist within the crystal structure, one surrounded by three fluorine and four oxygen atoms at distances between 2.294(2) and

*Department of Chemistry and Centre in Sustainable Chemical Technologies, University of Bath, Bath, BA2 7AY. E-mail: m.t.weller@bath.ac.uk. Tel: +44 (0) 1225 386531*

† *Electronic supplementary information (ESI) available. Experimental and calculated powder X-ray diffraction patterns for all phases reported, EDAX and AAS data for $Li_{1.87}Ti_{1.13}O_{0.39}F_{1.61}(SO_4)_2$. CIF and checkcif data for all phases.*

2.611(3) Å, and the other surrounded by two fluorine and five oxygen atoms at distances between 2.375(2) and 2.762(3) Å. [21]

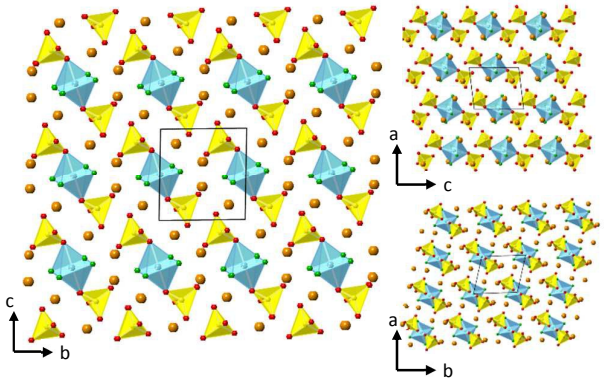


**Fig. 1** Crystal structure of $Na_4TiF_4(SO_4)_2$ viewed along the *a*- (left), *b*- (top right) and *c*- (bottom right) axes. Colour key: $TiF_4O_2$ octahedra in pale blue, $SO_4$ tetrahedra in yellow and Na, O and F atoms in orange, red and green respectively. The unit cell is outlined in black.

### (II) $[N_2C_{10}H_{10}]TiF_4SO_4$

Colourless, prismatic crystals of $[N_2C_{10}H_{10}]TiF_4SO_4$ were grown from the mixture of LiF (0.05199 g, 2 mmol), $H_2TiF_6$ (0.16mL, 1 mmol), $H_2SO_4$ (0.165 mL, 2.94 mmol) and 4,4'-bipyridine (0.15617 g, 1 mmol) treated hydrothermally at 200 °C for 72 hours. Visual phase purity of approximately 60% confirmed by PXRD. Compound **II** crystallises in the triclinic space group P-1 and contains discrete complex polyhedral units of composition $[(TiF_4SO_4)_2]^{4-}$. In each complex anion two cis-$TiF_4O_2$ octahedra are doubly bridged, through oxygen, by two $SO_4$ tetrahedra; discrete units. As with $Na_4TiF_4(SO_4)_2$ the discrete units align linearly above one another along all three unit cell directions, and the doubly protonated 4,4'-bipyridyl cations hydrogen bond with terminal oxide and fluoride ions with N-H…O/F distances of 2.04(5) to 2.38(4) Å.

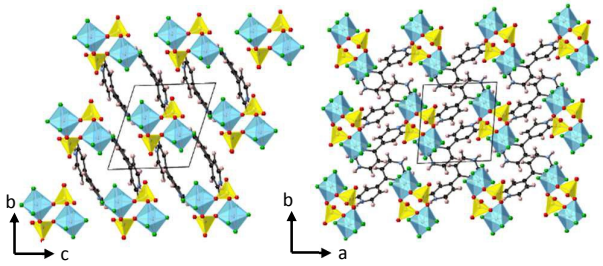


**Fig. 2** Crystal structure of $[N_2C_{10}H_{10}]TiF_4SO_4$ viewed along the *a*- and *c*- axes (left and right respectively). Colour key: $TiF_4O_2$ octahedra in pale blue, $SO_4$ tetrahedra in yellow and O, F, C, N and H atoms in red, green, black, blue and pale pink respectively. The unit cell is outlined in black.

### (III) $K_2FeF_3SO_4$

Yellow, columnar crystals of $K_2FeF_3SO_4$ were grown from the mixture of $FeC_2O_4$ (0.0532 g, 0.37 mmol), $H_2SO_4$ (0.0804 ml, 1.479 mmol) and KF (0.0859 g, 1.479 mmol) treated hydrothermally at 175 °C for 48 hours. Visual phase purity of approximately 10% confirmed by PXRD. Compound **III** crystallises in the orthorhombic space group *Pbcn* and comprises of one dimensional chains of interconnected $FeF_4O_2$ octahedra and $SO_4$ tetrahedra with potassium cations in the inter-chain space. The chains are formed from interlinked Fe-centres bridged by $\mu^2$-F atoms and vertex sharing $SO_4$ polyanions with the *trans*-O atoms of the $FeF_4O_2$ octahedra of the two nearest neighbour Fe centres. The remaining two fluoride ions of the $FeF_4O_2$ octahedra are oriented towards the inter chain space and form the coordination environment of the potassium cation along with the two free oxygen atoms of the $SO_4$ tetrahedra, with the K-O/F distances between 2.678(1) and 2.912(1) Å.

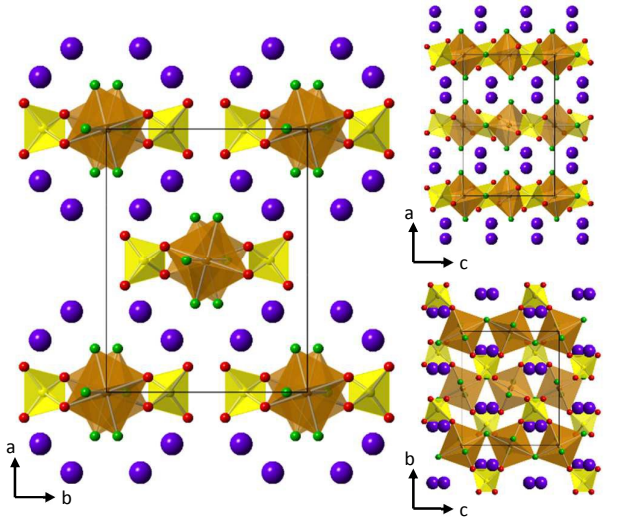


**Fig. 3** Crystal structure of $K_2FeF_3SO_4$ viewed along the *c*- (left), *b*- (top right) and *a*- (bottom right) axes. Colour key: $FeF_4O_2$ octahdra in brown, $SO_4$ tetrahedra in yellow and O, F, K atoms in red, green and purple respectively. The unit cell is outlined in black.

### (IV) $Li_{1.87}Ti_{1.13}O_{0.39}F_{1.61}(SO_4)_2$

Colourless, tablet shaped crystals of $Li_{1.87}Ti_{1.13}O_{0.39}F_{1.61}(SO_4)_2$ were grown from a mixture of $H_2TiF_6$ (0.16 mL, 1 mmol), $Li_2SO_4$ (0.2554 g, 2.32 mmol) and $H_2SO_4$ (0.16 mL, 2.85 mmol) treated hydrothermally at 210 °C for 72 hours. Initial visual phase purity of approximately 40%, further stoichiometric reactions (5:5:5 mmol equivalents of reagents) gave 100% phase purity confirmed by PXRD. Compound **IV** crystallises in the orthorhombic space group *Cmca* and initially solved to the idealised composition $Li_2TiF_2(SO_4)_2$. The structure comprises of one dimensional chains of interconnected *trans*-$TiO_4F_2$ octahedra and $SO_4$ tetrahedra with octahedrally coordinated $Li^+$ cations in the inter chain space (Fig. 4). These *cis*-$LiO_4F_2$ octahedra (Li-O/F distances of 2.025(3) Å to 2.092(3) Å) face share in the a-direction along with the titanium fluoride sulphate chains. A closer inspection of the $Li^+$ cation site revealed some excess electron density which was attributed to partial substitution of $Li^+$ by the similarly sized $Ti^{4+}$ cation. This disorder was modelled and refined to give a Li:Ti ratio of 93:7. A lithium-poor composition, relative to the idealised stoichiometry $Li_2TiF_2(SO_4)_2$, was also confirmed by Li atomic absorption spectroscopy (AAS) and EDAX, see ESI. The resulting excess positive charge was balanced by partial

substitution of $O^{2-}$ anions at the terminal $F^-$ anion site, with an F:O ratio of 81:19. This substitutional disorder generates a small level of three dimensional nature to the structure as the chains become cross linked in the *bc* plane wherever $Ti^{4+}$ replaces $Li^+$. This in turn may increase the rigidity of the material to lithium intercalation or deintercalation.

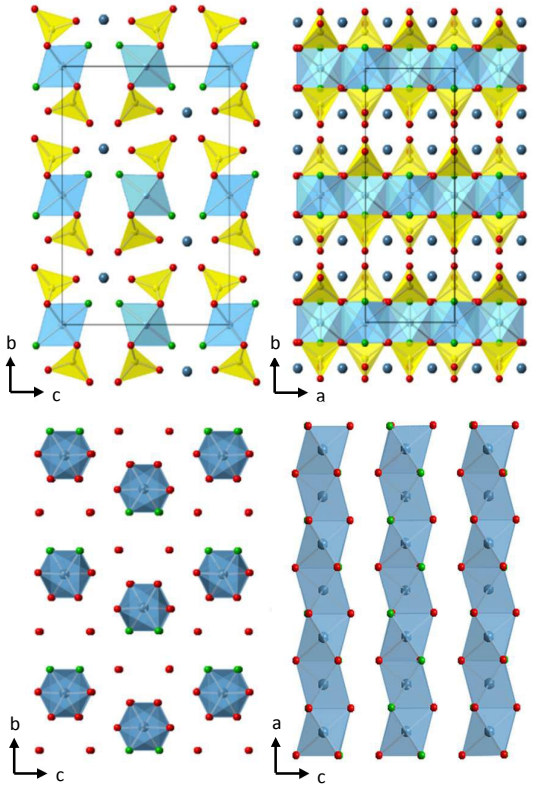


**Fig. 4** Crystal structure of $Li_2TiF_2(SO_4)_2$ viewed along the *a*- and *c*- axes (top left and right respectively), Bottom left and right show the face charing chains of $LiO_4F_2$ octahdra as viewed along the *a*- and *b*- axes respectively. Colour key: $TiO_4F_2$ octahedra in pale blue, $SO_4$ tetrahedra in yellow and O, F and Li atoms/octahedra in red, green and mid blue respectively. The unit cell is outlined in black.

### (V) $[N_2C_{10}H_{12}]TiF_2(SO_4)_2$

Colourless, rod-shaped crystals of $[N_2C_{10}H_{12}]TiF_2(SO_4)_2$ were grown from the mixture of NaF (0.0890 g, 2.12 mmol), $H_2TiF6$ (0.16mL, 1 mmol), $H_2SO_4$ (0.165 mL, 2.94 mmol) and 4,4'-bipyridine (0.15630 g, 1 mmol) treated hydrothermally at 200 °C for 72 hours. Visual phase purity of approximately 10-20% confirmed by PXRD. Compound **V** crystallises in the triclinic space group *P*-1 and comprises of one dimensional chains of inter connected $TiO_4F_2$ octahedra and $SO_4$ tetrahedra with doubly protonated 4,4'bipyridyl molecular cations in the inter-chain space. Similarly to compound **IV** the chains in compound **V** are formed from the bridging of trans-$TiO_4F_2$ octahedra by two $SO_4$ tetrahedra infinitely along the *a* cell direction, but instead of lithium cations in the inter-chain space there are doubly protonated 4,4'bipyridyl molecular cations which form hydrogen bonds with terminal oxygens of the $SO_4$ tetrahedra with an H…O distance of 1.89(3) Å. This hydrogen bonding directs the packing arrangement of the chains with respect to the molecular cations as seen in Fig. 5.

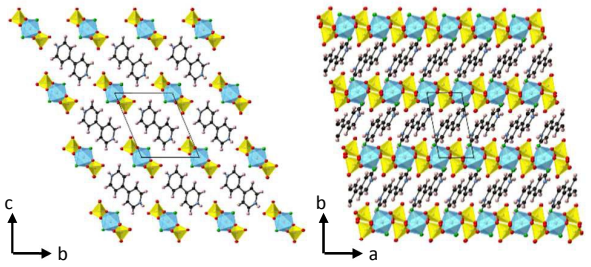


**Fig. 5** Crystal structure of $[N_2C_{10}H_{12}]TiF_2(SO_4)_2$ viewed along the *a*- and *c*- axes (left and right respectively). Colour key: $TiO_4F_2$ octahedra in pale blue, $SO_4$ tetrahedra in yellow and O, F, C, N and H atoms in red, green, black, blue and pale pink respectively. The unit cell is outlined in black.

### (VI) $Li_3FeF_2(SO_4)_2{\cdot}H_2O$

Opaque, yellow-green, needle-shaped crystals of $Li_3FeF_2(SO_4)_2{\cdot}H_2O$ were grown from the mixture $FeF_3$ (0.1 g, 0.599 mmol), $H_2SO_4$ (0.0652 ml, 1.198 mmol) and $LiOH{\cdot}H_2O$ (0.0776 g, 1.797 mmol) treated hydrothermally at 175 °C for 48 hours. Visual phase purity of approximately 60% confirmed by PXRD. Compound **VI** crystallises in the monoclinic space group $P2_1/n$ and comprises of one dimensional chains of interlinked $FeO_4F_2$ octahedra and $SO_4$ tetrahedra with lithium ions and water molecules on the inter-chain space. Relatively poor refinement statistics were obtained for this structure and these can

be attributed to the needle shaped crystals and one dimensional nature of the crystal structure which indicated some positional disorder of the parallel chains and neighbouring water molecules.

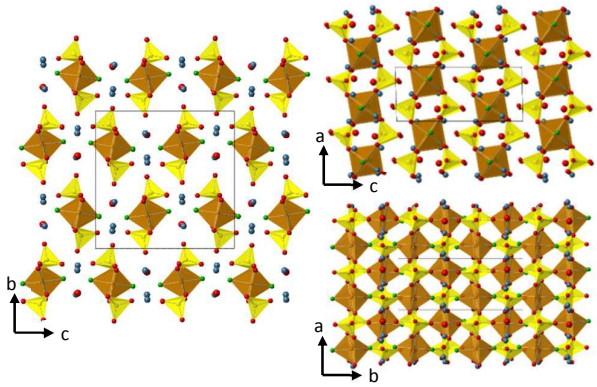


**Fig. 6** Crystal structure of $Li_3FeF_2(SO_4)_2{\cdot}H_2O$ viewed along the *a*- (left), *b*- (top right) and *c*- (bottom right) axes. Colour key: $FeO_4F_2$ octahedra in brown, $SO_4$ tetrahedra in yellow and O, F and Li atoms in red, green and mid blue respectively. The o atom of the water molecule is shown as a similar sized sphere to the Li and the unit cell is outlined in black.

Similarly to compounds **IV** and **V,** the infinite chains present in compound **VI** are formed from the bridging of *trans*-$MO_4F_2$ octahedra by two $SO_4$ tetrahedra along the *a* cell direction. The additional lithium cations and inter-chain water molecules result in a more open packing of these chains within the unit cell in comparison with compound **IV**. The hydrogen atom positions of the inter-chain water molecule could not be determined from the SXD

data but inspection of the atoms closet to the oxygen atom site shows three different terminal oxygen atom sites from $SO_4$ tetrahedra at O…O distances between 2.916(4) and 2.963(4) Å, which would suggest hydrogen bonding beween the water molecule and these terminal oxygens of the sulfate groups on the chains.

**(VII+VIII) $[N_2C_6H_{16}]MF(SO_4)_2$ (M=Fe,V)**

Dark brown needle crystals of $[N_2C_6H_{16}]FeF(SO_4)_2$ were grown from the mixture of $FeF_2$ (0.067 g, 0.714 mmol), $H_2SO_4$ (0.1553 ml, 2.856 mmol) and *trans*-1,4-diaminocyclohexane (0.1631 g, 1.42 mmol) treated hydrothermally at 175 °C for 48 hours. Visual phase purity of approximately 75% confirmed by PXRD. Dark green needle-shaped crystals of $[N_2C_6H_{16}]VF(SO_4)_2$ were grown from the mixture of $VF_3$ (0.0432 g, 0.4 mmol), $H_2SO_4$ (0.0871 ml, 1.9 mmol) and *trans*-1,4-diaminocyclohexane (0.0914 g, 0.95 mmol) treated hydrothermally at 175 °C for 48 hours. Visual phase purity of approximately 20%. Both Fe and V forms of $[N_2C_6H_{16}]MF(SO_4)_2$ crystallise in the monoclinic space group $P2_1/c$ and comprise of one dimensional chains of interconnected $MO_4F_2$ octahedra and $SO_4$ tetrahedra with doubly protonated *para*-diaminocyclohexane molecular cations in the inter-chain space.

The inorganic chains are formed from vertex sharing *trans*-$MO_4F_2$ octahedra, each further connected to its nearest neighbour via vertex sharing with two $SO_4$ tetrahedra. The only terminal atoms are the remaining two oxygen atoms of the $SO_4$ tetrahedra, which are oriented towards the inter-chain space and form hydrogen bonds with the protonated $NH_3$ groups on the diaminocyclohexane molecular cations at O....H-N distances of 2.051(60) Å and 2.495(62) Å. This interaction gives rise to the alternate stacking of the chains within the unit cell as seen in Fig. 7.

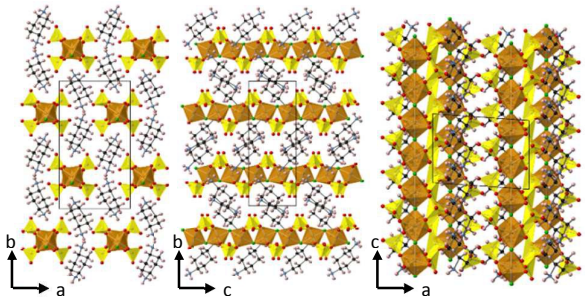


**Fig. 7** Crystal structure of $[N_2C_6H_{16}]FeF(SO_4)_2$ viewed along the *c*-, *a*- and *b*- axes (left to right). Colour key: $FeO_4F_2$ octahedra are shown in brown, $SO_4$ tetrahedra in yellow and O, F, C, N and H atoms in red, green, black, blue and pale pink respectively. The unit cell is outlined in black.

**(IX) $[N_2C_6H_{16}]_2Mn_3(H_2O)_2F_2(SO_4)_4$**

Pale pink, rod-shaped crystals of $[N_2C_6H_{16}]_2Mn_3(H_2O)_2F_2(SO_4)_4$ were grown from the mixture of $MnF_3$ (0.0532 g, 0.475 mmol), $H_2SO_4$ (0.1034 ml, 1.9 mmol) and *trans*-1,4-diaminocyclohexane (0.1085 g, 0.95 mmol) treated hydrothermally at 150 °C for 48 hours. Visual phase purity of approximately 40% confirmed by PXRD. Compound **IX** crystallises in the monoclinic space group $P2/c$ and comprises of two dimensional layers of interconnected $MnO_4F(H_2O)/MnO_4F_2$ octahedra and $SO_4$ tetrahedra with doubly protonated *para*-diaminocyclohexane molecular cations in the inter-layer space.

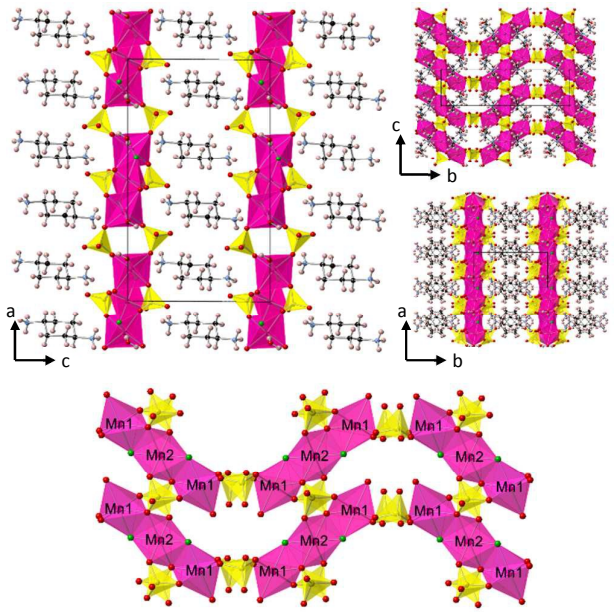


**Fig. 8** Crystal structure of $[N_2C_6H_{16}]_2Mn_3(H_2O)_2F_2(SO_4)_4$ viewed along the *b*-(left), *a*- (top right) and *c*- axes. Colour key $MnO_5F$ and $MnO_4F_2$ octahedra in pink, $SO_4$ tetrahedra in yellow and O, F, C, N and H atoms in red, green, black, blue and pale pink respectively. The unit cell is outlined in black. The bottom image shows the connectivity of the Mn centre triplets within the layers.

There are two distinct manganese environments within the layers which connect together in groups of three edge sharing octahedra (one *trans*-$MnO_4F_2$octahdra (O-F) edge shares with two *trans*-$MnO_4F(H_2O)$ octahedra). These groups of three octahedra are further interconnected by two distinct $SO_4$ tetrahedra: one of which vertex shares two oxygen atoms between two *trans*-$MnO_4F(H_2O)$ octahedra with its remaining two terminal oxygen atoms oriented into the interlayer space thereby forming hydrogen bonds with the protonated N-atoms of the *para*-diaminocyclohexane at O…H distances of 1.90(4) and 1.95(3) Å. The other sulfate group vertex shares three oxygen atoms between four Mn centres such that this $SO_4$ tetrahedron bridges two oxygen atoms on *trans*-$MnO_4F(H_2O)$ octahedron and a *trans*-$MnO_4F_2$ octahedra on one trimer of Mn centres, and one oxygen atom that is bridging between a *trans*-$MnO_4F(H_2O)$ octahedron and a *trans*-$MnO_4F_2$ octahderon on an adjacent trimer; the remaining oxygen atom of this sulfate group is oriented towards the inter layer space and a protonated nitrogen atom of a *para*-diaminocyclohexane molecular cation at a O…H distance of 2.70(3) Å.

**(X) $Na_2VF_3SO_4$**

Dark forest-green, prismatic crystals of $Na_2VF_3SO_4$ were grown from the mixture of NaOH (0.64 mL, 12 mmol), $VF_3$ (0.4317 g, 4 mmol) and $H_2SO_4$ (0.45 mL, 8 mmol) treated hydrothermally at 175 °C for 48 hours. The dried sample contained two distinct phases, bright

green crystals identified as $Na_3VF_2(SO_4)_2$[15] and the dark forest green crystals identified as Compound **X**. Initial phase purity was approximately 10% but further attempts to obtain pure phase samples have increased this to 65% (reactant ratio 9:6:6 mmol NaOH:$VF_3$:$H_2SO_4$ hydrothermally treated at 190 °C for 2 days), this was confirmed by PXRD. Compound **X** crystallises in the triclinic space group *P*-1 and comprises of two dimensional layers of interconnected *trans*-$VF_4O_2$ octahedra and $SO_4$ tetrahedra with sodium cations in the inter-layer space. The layers are formed from the interconnectivity of chains of vertex sharing *trans*-$VF_4O_2$ octahedra interlinked by $SO_4$ tetrahedra. The terminal oxide anions of the $SO_4$ tetrahedra are oriented towards the inter layer space and together with the two terminal fluoride anions of the *trans*-$VF_4O_2$ octahedra form the seven and eight fold coordination environments of the two crystallographically distinct Na cation sites at Na-F/O distances between 2.265(2) and 2.485(2) Å.

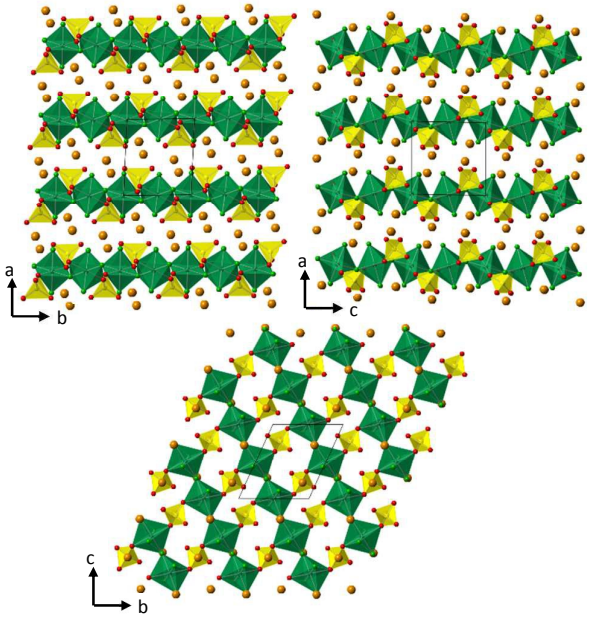


**Fig. 9** Crystal structure of $Na_2VF_3SO_4$ viewed along the *c*-, *b*- and *a*- axes (clockwise from top left). Colour key: $VF_4O_2$ octahedra in forest green and $SO_4$ tetrahedra in yellow and O, F and Na atoms in red, green and orange respectively. The unit cell is outlined in black.

### (XI) $Na_3CrF_2(SO_4)_2$

Green, prismatic crystals of $Na_3CrF_2(SO_4)_2$ were grown from the mixture of $CrF_3$ (0.10919 g, 1 mmol), NaF (0.08379 g, 2 mmol), $H_2SO_4$ (0.220 mL, 4 mmol) and HF (0.05 mL, 1.4 mmol) treated hydrothermally at 180 °C for 96 hours. Visual phase purity very low, as crystals grow in an amorphous green solid. Compound **XI** crystallises in the orthorhombic space group *Pbcn* and comprises of two dimensional layers of interconnected *cis*-$CrO_4F_2$ octahedra and $SO_4$ tetrahedra with sodium cations in the inter-layer space. As seen previously for the isostructural $Na_3MF_2(SO_4)_2$ (M = Fe, V and Mn)[15] the $CrO_4F_2$ octahedra vertex share all four oxygen atoms with four $SO_4$ tetrahedra. Each $SO_4$ tetrahedra shares two oxygen atoms with two $CrO_4F_2$ octahedra with the remaining two oriented towards the inter layer space and $Na^+$ cations. The two *cis*-fluorine atoms on each Cr-centre are oriented towards the interlayer space such that each polyhedron's four nearest neighbour fluorine atoms are on the opposite sides of the layer. There are two distinct coordination environments for the $Na^+$ cations within the inter layer space: one trigonal prismatic $NaO_2F_4$ and one irregular seven-fold $NaO_6F$ with the shortest Na-Na distance of 3.436(2) Å. An inspection of the Cr-F/O distances as shown in Fig. 10 confirm regular octahedral geometry as found with the V and Fe analogues previously. This is contrast to the Mn analogue which shows Jahn-Teller distortion with elongated axial Mn-O bonds.

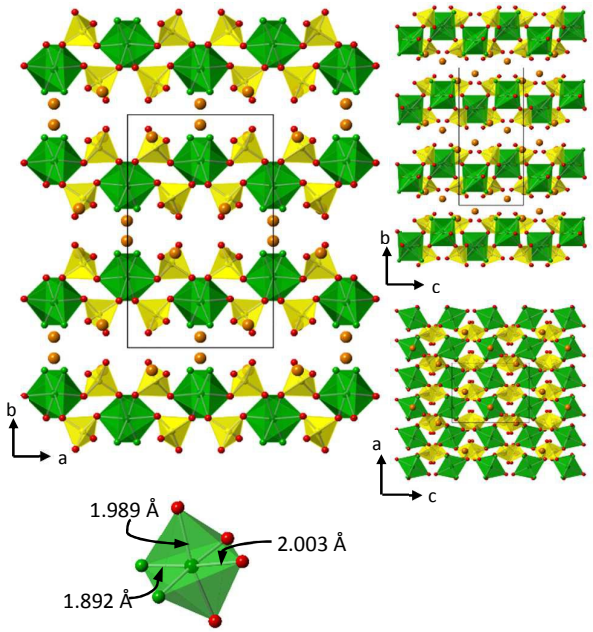


**Fig. 10** Crystal structure of $Na_3CrF_2(SO_4)_2$ viewed along the *c*- (left), *a*- (top right) and *b*- (bottom right) axes. The bottom right image shows a $CrO_4F_2$ octahedra with CR-O/F bond distances. Colour key: $CrO_4F_2$ octahedra in bright green, $SO_4$ tetrahedra in yellow and O,F and Na atoms in red, green and orange respectively. The unit cell is outlined in black.

### Overall discussion

The results reported here summarise the new phases found in this study. Many further reactions were undertaken during this work in the search for novel phases. The area is systematically investigated by selecting high fluoride-content precursors such as LiF/NaF in combination with transition metal fluorides, and low oxygen/water content reactants. A full range on molar ratios between the metal and oxoanion from 1:5 to 1:1 was surveyed. The pH of the reaction mixture was also controlled; in the case of titanium, $H_2TiF_6$ was used when low levels of sulfuric acid were employed, thus increasing the acidity of the reaction mixture without decreasing the Ti:$SO_4$ ratio.

The choice of anhydrous iron oxalate as the precursor for $K_2FeF_3SO_4$ arose from the requirement to reduce the amount of water present in the reaction mixture as OH will often competitively bind to transition metals instead of F.

Aside from the new phases, many other reactions gave mixtures of products that were identified by PXRD as previously reported in the literature; these products included

alkali metal sulfates, transition metal sulfates and oxides. Generally, a slight excess of $H_2SO_4$ was employed compared to the transition metal source with the aim of achieving a fluid reaction media containing as little water as possible. When small levels of a novel phases was discovered in the reaction product, efforts to improve phase purity were undertaken by adjusting reactant ratios, reaction times and temperatures. These optimised reaction conditions are reported in this work.

## Experimental

### Synthesis

All samples were prepared from commercially available materials of reagent grade with no need for further purification. The compounds were synthesised hydrothermally with reactions performed in 23mL Teflon™-lined Parr autoclaves, with the reaction compositions and conditions as stated in each structure description. **Warning!** Caution should be taken due to the potentially violent nature of the reactions, with generation of HF gas (very toxic by inhalation, in contact with skin and if swallowed) as a side product. Products, collected by filtration, were washed with deionised water and dried in air at 80 °C overnight. Single crystal specimens were removed from samples before being ground and analysed via PXRD to check phase purity.

### X-ray diffraction studies

Single-crystal X-ray diffraction (SXRD) data were collected at 150 K for structures **VII**, **IX** and **XI** on a SuperNova dual source EosS2 diffractometer operating Cu (λ = 1.5418 Å) radiation. Remaining SXD data were collected at 150 K on diffractometers operating Mo (λ = 0.7103 Å) as follows: structures **I**, **IV** and **VI** on a SuperNova dual source EosS2, structures **II**, **V** and **X** on an Xcalibur EosS2 and structures **III** and **VIII** on a Rigaku FR-E$^+$ ultra-high flux diffractometer. Structures were solved using the WinGX suite of programmes,[22] utilising XPREP[23] and SHELX-2013,[24] by direct methods. All non-hydrogen atomic displacement parameters were refined anisotropically, using the $F^2$ least-squares method. Assignment of sites as oxygen or fluorine was achieved using a combination of data fitting, charge balancing and bond valence calculations. In most instances, initial allocation of an oxide ion to an anion site yielded non-positive of very small ADP values if the anion site was fluoride and reassignment of this scattering power to fluoride provided similar ADP values for all anion site. Where ambiguities arose during ADP analysis, charge balancing considerations combined with bond valence calculations were implemented, with bond valence calculations readily distinguishing between the -1 and -2 charge on fluoride and oxide anions. For example, incorrect assignment of an anion site to oxide would yield very low bond valence calculations for this site, <1.3, indicating a fluoride ion in that position. As such amendments were made to the crystallographic models accordingly. Crystallographic database deposition information is provided under notes and references

Powder X-ray diffraction (PXRD) studies were carried out on a Siemens D5000 diffractometer operating Cu Kα radiation (λ = 0.154 nm) coupled to a scintillation counter detector. Samples were mounted on either aluminium or silicate glass holder then scanned in the 2θ range of 5-80° with a scan speed of 2° per minute at room temperature. Results are summarised in the ESI where experimental and calculated powder patterns are compared to demonstrate the purity of the as-synthesised materials.

## Conclusions

In conclusion, eleven new, early- to mid- first row, transition metal fluoride sulfate phases have been synthesised from a high fluoride hydrothermal synthetic procedure and structurally analysed using single crystal X-ray diffraction. A variety of templating and counter cations has been used to generate these materials ranging in size from lithium to protonated diaminocyclohexane. The connectivity within these phases varies greatly form discreet units, through one dimensional chains to two dimensional layers.

Perhaps of most interest for potential applications are those that incorporate the smaller cations $Li^+$ and $Na^+$ as these compounds could be employed as functional materials in Li-ion and Na-ion rechargeable batteries. For Na-ion batteries compound **X,** $Na_2V(III)F_3SO_4$, has a highly promising composition and structure with a layer-type structure from which two sodium ions could potentially be extracted to form $V(V)F_3SO_4$. Similar it would be chemically feasible to remove three sodium ions from compound **XI** $Na_3Cr(III)F_2(SO_4)_2$ to form the chemically well-known Cr(VI) in $CrF_2(SO_4)_2$. For lithium ion battery cathodes compound **V** $Li_3FeF_2(SO_4)_2{\cdot}H_2O$ containing Fe (III) could be potentially oxidized to $Fe^{3.5+}$ through lithium extraction and reduced to $Fe^{2+}$ through lithium insertion; however the presence of water in the structure may make oxidative delithiation impracticable.

For the compounds reported that contain larger and more complex counter cations the potential exists to ion exchange these species with $Li^+$ or $Na^+$ and thereby form more open structures of interest as battery cathode materials. The titanium compound **I,** $Na_4TiF_4(SO_4)_2$**,** contains a high level of sodium ions and these maybe highly mobile in the three dimensionally linked space between the complex titanosulfate cations. Such materials may be of interest either as electrolytes or anodes in a sodium ion battery.

Further work is planned to investigate the potential rechargeable battery applications for many of these new materials.

## Acknowledgements

The authors would like to thank the University of Bath for studentship funding for KLM and QW, and the EPSRC Doctoral Training Centre in Sustainable Chemical Technologies for M.Res. project funding for HSIS, (EP/G03768X/1). Thanks are also due to Alan Carver for the AAS analysis of compound **IV**.

## Notes and references

‡ *CCDC 1452167-CCDC 1452171 contains the supplementary crystallographic data for compounds **IX**, **VII**, **VIII**, **V** and **II**. The data can be obtained free of charge from The Cambridge Crystallographic Data Centre via www.ccdc.cam.ac.uk/structures. Further details of the crystal structure investigations of compounds **I**, **III**, **IV**, **VI**, **X** and **XI** may be obtained from FIZ Karlsruhe, 76344 Eggenstein-Leopoldshafen, Germany (fax: (+49)7247-808-666; e-mail: crysdata(at)fiz-karlsruhe(dot)de, on quoting the deposition numbers CSD-430826 to CSD-430831.*

1 A. K. Padhi, K. S. Nanjundaswamy and J. B. Goodenough, *J. Electrochem. Soc.*, 1997, **144**, 1188-1194.
2 P. Bonnet, J. M. M. Millet, C. Leclercq and J. C. Vedrine, *J. Catal.*, 1996, **158**, 128-141.
3 C. Masquelier and L. Croguennec, *Chem. Rev.*, 2013, **113**, 6552-6591.
4 S. T. Wilson, B. M. Lok, C. A. Messina, T. R. Cannan and E. M. Flanigen, *Journal of the American Chemical Society*, 1982, **104**, 1146-1147.
5 E. Ferg, R. J. Gummow, A. Dekock and M. M. Thackeray, *J. Electrochem. Soc.*, 1994, **141**, L147-L150.
6 O. García-Moreno, M. Alvarez-Vega, J. García-Jaca, J. M. Gallardo-Amores, M. L. Sanjuán and U. Amador, *Chemistry of Materials*, 2001, **13**, 1570-1576.
7 B. L. Ellis, W. R. M. Makahnouk, Y. Makimura, K. Toghill and L. F. Nazar, *Nature Materials*, 2007, **6**, 749-753.
8 M. Armand and J. M. Tarascon, *Nature*, 2008, **451**, 652-657.
9 R. Tripathi, S. M. Wood, M. S. Islam and L. F. Nazar, *Energy Environ. Sci.*, 2013, **6**, 2257-2264.
10 J. A. Armstrong, E. R. Williams and M. T. Weller, *Journal of the American Chemical Society*, 2011, **133**, 8252-8263.
11 J. A. Armstrong, E. R. Williams and M. T. Weller, *Dalton Transactions*, 2012, **41**, 14180-14187.
12 E. R. Williams, S. A. Morris and M. T. Weller, *Dalton Transactions*, 2012, **41**, 10845-10853.
13 J. A. Armstrong, E. R. Williams and M. T. Weller, *Dalton Trans.*, 2013, **42**, 2302-2308.
14 A. C. Keates, J. A. Armstrong and M. T. Weller, *Dalton Transactions*, 2013, **42**, 10715-10724.
15 Q. Wang, A. Madsen, J. R. Owen and M. T. Weller, *Chemical Communications*, 2013, **49**, 2121.
16 K. L. Marshall and M. T. Weller, *Z. Anorg. Allg. Chem.*, 2014, **640**, 2766-2770.
17 J. Rouse, K. V. Redrup, E. Kotsapa and M. T. Weller, *Chemical Communications*, 2009, 7209-7211.
18 S. Il Park, I. Gocheva, S. Okada and J.-i. Yamaki, *J. Electrochem. Soc.*, 2011, **158**, A1067-A1070.
19 A. Rudola, K. Saravanan, S. Devaraj, H. Gong and P. Balaya, *Chemical Communications*, 2013, **49**, 7451-7453.
20 H. Kang, Y. Liu, K. Cao, Y. Zhao, L. Jiao, Y. Wang and H. Yuan, *Journal of Materials Chemistry A*, 2015, **3**, 17899-17913.
21 M. M. G. a. D. L. Motov, *Zhunal Neorganic Khimii*, 2003, **44**, 741.
22 L. J. Farrugia, *Journal of Applied Crystallography*, 1999, **32**, 837-838.
23 G. Sheldrick, *XPREP, Space Group Determination and Reciprocal Space Plots*, 1991.
24 G. M. Sheldrick, *Acta Crytollagraphica Section A: Foundations of Crystallography*, 2008, **64**, 112-122.

**Table 1** Summary of the crystallographic information for all compounds

| Structure | Formula weight (g) | Crystal system | Space group | Unit cell dimensions (Å/°) | | Volume (Å$^3$) | Z | R indices all data | GOOF |
|---|---|---|---|---|---|---|---|---|---|
| **(I)** $Na_4TiF_4(SO_4)_2$ | 407.95 | Triclinic | *P*-1 | *a* = 5.5997(10)<br>*b* = 6.6012(12)<br>*c* = 6.6657(12) | α = 86.361(15)<br>β = 82.230(15)<br>γ = 74.777(16) | 235.47(8) | 1 | $R_1$= 0.040<br>$wR_2$= 0.096 | 1.093 |
| **(II)** $[N_2C_{10}H_{12}]$ $TiF_4SO_4$ | 330.1 | Triclinic | *P*-1 | *a* = 8.691(2)<br>*b* = 9.208(2)<br>*c* = 9.288(2) | α = 68.56(2)<br>β = 84.30(2)<br>γ = 81.59(2) | 683.6(3) | 2 | $R_1$= 0.103<br>$wR_2$= 0.133 | 1.039 |
| **(III)** $K_2FeF_3SO_4$ | 287.09 | Orthorhombic | *Pbcn* | *a* = 10.9902(4)<br>*b* = 8.4234(3)<br>*c* = 7.157 (3) | | 662.56(4) | 4 | $R_1$= 0.033<br>$wR_2$= 0.0817 | 1.08 |
| **(IV)** $Li_{1.87}Ti_{1.13}O_{0.39}F_{1.61}(SO_4)_2$ | 295.99 | Orthorhombic | *Cmca* | *a* = 5.1591(2)<br>*b* = 13.6978(4)<br>*c* = 9.4613(3) | | 668.74(4) | 4 | $R_1$= 0.031<br>$wR_2$= 0.080 | 1.166 |
| **(V)** $[N_2C_{10}H_{12}]TiF_2(SO_4)_2$ | 436.2 | Triclinic | *P*-1 | *a* = 4.5768(3)<br>*b* = 8.9162(6)<br>*c* = 10.1236(9) | α = 112.888(7)<br>β = 95.196(6)<br>γ = 98.706(5) | 371.11(14) | 1 | $R_1$= 0.045<br>$wR_2$= 0.081 | 1.054 |
| **(VI)** $Li_3FeF_2(SO_4)_2{\cdot}H_2O$ | 324.89 | Monoclinic | $P2_1/n$ | *a* = 5.173(2)<br>*b* = 12.592(5)<br>*c* = 12.273(5) | β = 91.647(9) | 799.08(6) | 4 | $R_1$= 0.0717<br>$wR_2$= 0.1905 | 1.086 |
| **(VII)** $(N_2C_6H_{14})Fe(SO_4)_2F$ | 383.2 | Monoclinic | $P2_1/c$ | *a* = 10.2220(3)<br>*b* = 17.6599(4)<br>*c* = 7.0437(2) | β = 93.894(2) | 1268.59(2) | 4 | $R_1$= 0.042<br>$wR_2$= 0.122 | 1.072 |
| **(VIII)** $(N_2C_6H_{14})V(SO_4)_2F$ | 374.24 | Monoclinic | $P2_1/c$ | *a* = 10.262(2)<br>*b* = 17.761(4)<br>*c* = 7.052(2) | β = 93.935(7) | 1282.2(5) | 4 | $R_1$= 0.0661<br>$wR_2$= 0.1858 | 0.959 |

| | | | | | | | | | |
|---|---|---|---|---|---|---|---|---|---|
| **(IX)** $[N_2C_6H_{16}]_2Mn_3(H_2O)_2F_2(SO_4)_4$ | 570.34 | Monoclinic | *P*2/*c* | *a* = 12.0101(5)<br>*b* = 5.6681(2)<br>*c* = 20.4103(8) | β = 90.425(4) | 1389.38(1) | 3 | $R_1$= 0.029<br>$wR_2$= 0.060 | 1.003 |
| **(X)** $Na_2VF_3SO_4$ | 250.0 | Triclinic | *P*-1 | *a* = 6.3555(5)<br>*b* = 6.4255(8)<br>*c* = 7.3724(7) | α = 65.119(11)<br>β = 89.696(7)<br>γ = 86.853(8) | 272.66(15) | 2 | $R_1$ = 0.031<br>$wR_2$ = 0.063 | 1.112 |
| **(XI)** $Na_3CrF_2(SO_4)_2$ | 351.1 | Orthorhombic | *Pbcn* | *a* = 8.7463(5)<br>*b* = 13.8814(7)<br>*c* = 6.6009(3) | | 801.42(1) | 4 | $R_1$= 0.049<br>$wR_2$= 0.128 | 1.046 |

Eleven new transition metal fluorosulfate structures have been synthesised and structurally characterised. These materials show a variety of polyanionic motifs ranging from discrete $[TiF_4(SO_4)_2]^{4-}$ polyanions (right) to complex layers.